Environ. Sci. Technol. **2003**, *37,* 1535−1544

Desorption Kinetics for Field-Aged Polycyclic Aromatic Hydrocarbons from Sediments

LESLIE M. SHOR,[†] KARL J. ROCKNE,[‡] GARY L. TAGHON,[§] L. Y. YOUNG,[||] AND DAVID S. KOSSON*,[†]

Department of Civil and Environmental Engineering, Vanderbilt University, Nashville, Tennessee 37235, Department of Civil and Materials Engineering, University of Illinois at Chicago, Chicago, Illinois 60607, and Institute of Marine and Coastal Sciences and Biotechnology Center for Agriculture and the Environment, Rutgers, The State University of New Jersey, New Brunswick, New Jersey 08901

This study considers desorption kinetics for 12 field-aged polycyclic aromatic hydrocarbons (PAHs) desorbing from size- and density-fractionated sediments collected from two locations in the New York/New Jersey Harbor Estuary. Desorption kinetics for PAHs with a log octanol−water partition coefficient greater than 6 were well-described by a one-domain diffusion model that assumes that PAHs are initially uniformly distributed throughout spherical sediment aggregates. PAH hydrophobicity and sediment specific surface area were the parameters most strongly correlated with the magnitude of the observed diffusivity for the one-domain model. For less hydrophobic PAHs, a two-domain desorption model was used also, and the results suggest that a substantial fraction of these field-aged PAHs desorb via a relatively fast macro-mesopore diffusion mechanism. The model-predicted fraction of PAHs in the fast-diffusion regime by compound and sediment was highly correlated with the measured percent PAH desorption in 24 h. The fast-domain diffusivity was 100 times greater than the slow-domain diffusivity, was correlated with both PAH properties and sediment physical and chemical properties, and could be estimated by readily obtainable physical and chemical parameters. In contrast, the slow-domain diffusivity was not significantly correlated with PAH properties. Our results suggest that macro-mesopore diffusion may control mass transport of less-hydrophobic PAHs in estuarine sediments.

Introduction

According to estimates by the U.S. Environmental Protection Agency, chemical contamination is severe enough in 10% of the sediments underlying U.S. surface waters to pose a potential risk to human health and the environment (*1*). Given the scope of the problem and the high cost of managing contaminated sediment, it is necessary to prioritize contaminated sediment management on the basis of comparative risk. The success of this approach is predicated on accurate prediction of contaminant mobility, availability, and toxic potency from a given matrix. Because of the large variability of a soil or sediment's capacity to sequester hydrophobic pollutants such as polycyclic aromatic hydrocarbons (PAHs) and decreased bioavailability and extractability with aging (*2*−*4*), contaminant concentration alone is insufficient to predict risk to humans and the environment.

Desorption of PAHs from natural soil or sediment depends on the contributions of many interconnected factors (see, for example, refs *5* and *6* for reviews). For example, it has been postulated that slow desorption of organic contaminants may be controlled by hindered diffusion through micropores or by slow diffusion through soil−sediment organic matter (SOM) (*6*−*9*). Several reports examining pore diffusion versus organic matter diffusion mechanisms have concluded that the presence of hydrophobic regions within the physical matrix have the largest impact on sorption, desorption, and bioavailability (*9*−*11*). Specific properties of SOM, such as the presence of detrital plant debris, have been shown to have a dramatic effect on observed rate and extent of PAH desorption in density-fractionated natural sediments (*12*).

Some researchers have postulated that desorption of hydrophobic organic contaminants (HOCs) in sediments may be limited by diffusion through condensed organic matter regions below the glass transition temperature (*13*). One study estimated that the observed diffusivity of small PAHs (e.g., phenanthrene) in coal-derived particles was on the order of 10^{-17} cm^2 s^{-1}, depending on the assumptions of the model (*14*). This observed diffusivity is more than 10 orders of magnitude smaller than the estimated free diffusivity of phenanthrene in water (*15*, *16*). While the vast majority of HOC mass is sequestered in SOM within sediment aggregates (e.g., phenanthrene log K_{oc} = 4.3; *17*), the large difference between aqueous-phase and SOM-phase diffusivities may allow for PAH diffusion through the water-filled macro-mesopore network to increase substantially the overall observed rate of mass transport. This may be especially true for less hydrophobic PAHs.

The purpose of this study was to better understand how SOM properties and sediment physical structure affect mass transport of individual PAHs in weathered estuarine sediments. To control for the complexity and heterogeneity of natural sediments, our strategy was to fractionate and extensively characterize the study materials and to measure sequestration, partitioning, and desorption for several PAHs from several sediment fractions, each with a known distribution of physical and chemical properties. This approach limited variability and complexity as compared to whole sediment and also provided multiple points of comparison among PAHs and sediment fractions. In this study, desorption of individual PAH from the <63- and 63−125-μm size fractions of each of two study sediments are reported. Spherical diffusion models were used to fit the observed diffusivity to the desorption kinetics of as many as 12 PAHs desorbing from each of eight sediment size and density fractions. A limited number of these desorption kinetics appeared previously (*12*). This study presents further desorption data with mass transport modeling of the combined extensive data sets and provides correlations between observed diffusivities and various sediment and PAH properties to establish the influence of various parameters on rate, extent, and mechanism of PAH mass transport from sediments. These analyses provide the phenomenological foundation for the development of a two-domain macro-

* Corresponding author phone: (615)322-1064; fax: (615)322-3365; e-mail: david.kosson@vanderbilt.edu.

[†] Vanderbilt University.

[‡] University of Illinois at Chicago.

[§] Institute of Marine and Coastal Sciences, Rutgers.

[||] Biotechnology Center for Agriculture and the Environment, Rutgers.

10.1021/es025734l CCC: $25.00
Published on Web 03/11/2003

mesopore and organic matter (MOM) diffusion model to describe desorption of field-aged PAHs from estuarine sediments.

Materials and Methods

Physical and Chemical Characterization of Study Sediments. Field-contaminated sediments were collected from Newtown Creek (NC) and Piles Creek (PC), both in the New York/New Jersey Harbor Estuary. These sediments were selected because both study sites have a long history of PAH contamination but have very different physical and chemical characteristics. Details on the study sediments, sediment separation methods, characterization and desorption techniques, and PAH quantification methods are given elsewhere (*12*). Briefly, each study sediment was fractionated by wet sieving into five size fractions (>500, 500−300, 300−125, 125−63, and <63 μm) and further separated into binary density fractions by equilibrium settling in a concentrated CsCl solution (less than or greater than 1.7 g mL^{-1}). By comparing PAH concentrations before and after size or density separation, the sediment fractionation procedures were determined not to remove PAHs. Whole sediment and sediment size and density fractions were extensively characterized for particle size distribution, specific surface area, pore size distribution, PAH concentration, total carbon and soot carbon concentrations, nitrogen concentration, and equilibrium sediment−water partitioning as reported previously (*12*). Sediment PAH concentration was determined by a hot acetonitrile extraction procedure wherein dewatered (centrifugation at 8000*g*) wet sediment was refluxed in hot acetonitrile (85 °C, 2 h) in tightly sealed Teflon centrifuge tubes with sonication. In this study, "total PAHs" is defined as the extractable concentration using this hot acetonitrile extraction procedure.

Sediment−pore water partitioning coefficients (K_{sed-pw}, L kg^{-1}) were determined by finding the ratio of the sediment and pore water concentrations for individual PAHs at the saturated sediment liquid:solid ratio for both whole sediments. Pore water was separated from saturated sediments by centrifugation (5600*g*, 1 h). PAH concentrations in pore waters were too low to be measured directly and were concentrated by solid-phase extraction (SPE) prior to analysis. After separation from the sediment solids, pore waters were amended with 10% methanol to enhance wetting and then drawn slowly (<1 mL min^{-1}) through 3-mL preconditioned (first methanol, then 10% water−methanol solution) LC-18 SPE tubes (Supelco, Bellefonte, PA). PAHs were eluted from the SPE tubes with 1 mL of acetonitrile and three portions of 0.5 mL of dichloromethane. The dichloromethane in the mixed solvent eluent was evaporated under a gentle N_2 stream, and the final volume of acetonitrile was established gravimetrically. Finally, PAHs in the concentrated SPE extract were analyzed by HPLC. This procedure resulted in greater than a 100-fold increase in the PAH concentration of the extract versus the PAH concentration in the pore water. The extraction efficiency of this procedure for ^{14}C-labeled pyrene in Nanopure water and a soil leachate was determined to be 86 ± 5% and 70 ± 33%, respectively (A. Oosterhoff, unpublished data). All solvents were HPLC grade.

PAH Desorption Kinetics. Desorption of PAHs was measured in duplicate for time periods up to 120 d by a modification of the Tenax shaken slurry desorption method of Cornelissen et al. (*18*) as described previously (*12*). Briefly, seawater and sediment slurries with Tenax-TA beads (60−80 mesh, Alltech Associates Inc., Deerfield, IL) were shaken (150 rpm, 23 °C) in closed glass separatory funnels. At time intervals, the slurry was transferred into another vessel with unused Tenax, and PAHs in the used Tenax were chemically extracted with hexane. The sum of the masses of individual PAHs desorbed at each transfer time plus the residual PAH mass remaining in the sediment was 95 ± 20% of the starting sediment concentration (as determined by hot acetonitrile extraction of split samples).

Analysis of PAHs by HPLC. Analytes in extracts of sediment, SPE tubes, and Tenax were separated by reverse-phase HPLC with a 40-min isothermal (35 °C) acetonitrile−water solvent gradient program using a 15-cm LC-PAH column (Supelco, Bellefonte PA), and quantified by photodiode array detection (Shimadzu Instruments SPD-M10AVP) or programmable fluorescence detection (Shimadzu Instruments model RF-10AXL). The basis of selection for the PAHs included in the study was that (i) they are all EPA priority PAHs and (ii) they were each consistently quantifiable with good replication and low procedural or analytical error.

Data Analysis. Diffusion models were used to fit the observed diffusivities to duplicate desorption kinetics data independently for each PAH and each sediment fraction. Depending on the number of time points in the desorption study, there were between 18 and 22 observations used for the model fits (except the 63−125 μm NC data series, which had 11 observations). The best-fit adjustable parameter value(s) were found using a macro written in Microsoft Excel (Microsoft Corp., Redmond, WA; Version 9.0) utilizing the solver function, which minimized the sum of squared differences between predicted and observed values. Statistical analyses were based on ordinary least-squares linear regression with intercept for the indicated dependent and independent variables. The statistical significance of the slope term (or *p* value) was computed using a one-tailed student's *t*-test. Significant correlations are defined as $p < 0.05$.

Model Development

One-Domain Diffusion Model. Intra-aggregate mass transport of hydrophobic contaminants from soil or sediment frequently has been modeled as a Fickian diffusion process (*10, 14, 19−26*). Fick's second law of diffusion in spherical coordinates is

$$\frac{\partial C}{\partial t} = D_{obs}\left(\frac{\partial^2 C}{\partial r^2} + \frac{2}{r}\frac{\partial C}{\partial r}\right) \quad (1)$$

where C (mg kg^{-1}) is the PAH concentration in the solid phase, t (s) is time, D_{obs} (cm^2 s^{-1}) is the observed diffusion coefficient, and r (cm) is the radial distance from the particle center. By making the substitution $u = Cr$, eq 1 becomes

$$\frac{\partial u}{\partial t} = D_{obs}\left(\frac{\partial^2 u}{\partial r^2}\right) \quad (2)$$

Initially, PAHs are assumed to be uniformly distributed throughout sediment aggregates. After the start of the desorption experiment, the surface concentration of the sediment aggregates is assumed to be very close to zero because the Tenax beads act as an "infinite sink". Therefore, the initial and boundary conditions are $u = 0$ for $r = 0$ and $t > 0$; $u = 0$ for $r = a$ and $t > 0$; $u = C_1 r$ for $0 < r < a$ and $t = 0$ (where C_1 is the initial PAH concentration distribution and a is the particle radius). Under these conditions, eq 2 has an analytical solution (*27*):

$$\frac{M(t)}{M(\infty)} = 1 - \frac{6}{\pi^2}\sum_{n=1}^{\infty}\frac{1}{n^2}\exp(-D_{obs}n^2\pi^2 t/\bar{a}^2) \quad (3)$$

where $M(t)/M(\infty)$ (dimensionless) is the fractional PAH mass desorbed with time [$M(\infty)$ is operationally defined as the total PAH mass desorbed after approximately 3 months]. Rao et al. (*28*) determined that a single representative size parameter, the volume-weighted equivalent spherical average aggregate radius ($\bar{a}$) could be used to accurately model solute diffusion from mixtures of many-sized aggregates. Therefore,

$\bar{a}$ is substituted for a in eq 3. Values for $\bar{a}$ were computed a priori from particle size distribution data (reported previously; *12*) for each sediment and sediment fraction and are tabulated in Table S1 of the Supporting Information. The sole adjustable parameter (D_{obs}) was estimated by fitting eq 3 to the experimental data for each PAH desorbing from each sediment fraction.

Macro-Mesopore and Organic Matter (MOM) Diffusion Model. Desorption of HOCs from natural materials can be described as a two-domain process: the first domain is rapid, linear, and reversible; and the second is slow, nonlinear, and nonreversible (*29*, *30*). Following the approach of previous reports (*21*, *31*), two-domain desorption can be modeled as a weighted linear combination of fast and slow diffusive processes:

$$\left.\frac{M(t)}{M(\infty)}\right|_{total} = f\left.\frac{M(t)}{M(\infty)}\right|_{fast} + (1-f)\left.\frac{M(t)}{M(\infty)}\right|_{slow} \quad (4)$$

where f is the fraction of PAHs in the fast diffusion domain. Substituting eq 3 into eq 4:

$$\frac{M(t)}{M(\infty)} = f\left(1 - \frac{6}{\pi^2}\sum_{n=1}^{\infty}\frac{1}{n^2}\exp(-D_{obs\,f}n^2\pi^2 t/\bar{a}^2)\right) + (1-f)\left(1 - \frac{6}{\pi^2}\sum_{n=1}^{\infty}\frac{1}{n^2}\exp(-D_{obs\,s}n^2\pi^2 t/\bar{a}^2)\right) \quad (5)$$

This two-domain model contains three adjustable parameters: the fast- and slow-domain observed diffusivities ($D_{obs\,f}$ and $D_{obs\,s}$) and the fraction (f) of desorbable PAHs in the fast-diffusion domain.

In addition to finding mass transport parameters to summarize desorption kinetics data, another purpose of modeling is to test and advance our understanding of the mechanisms controlling desorption of HOCs from sediments. Although we are never certain that a good fit between model and data means a correct mechanistic interpretation, this is even more the case for models with multiple adjustable parameters. Here, a means of predicting the fast-domain diffusivity ($D_{obs\,f}$) and the fraction in the fast diffusion domain (f) is proposed. The mechanistic foundation for $D_{obs\,f}$ is consistent with linear sediment−pore water partitioning and aqueous-phase diffusion in intra-aggregate sediment mesopores and macropores. As many previous studies have shown (*8*, *10*, *19*, *20*, *22*, *25*, *32*−*34*), observed diffusivity for a chemical species moving through a porous material can be related back to the free aqueous diffusivity (D_{mol}; $cm^2\ s^{-1}$) by accounting for the physical and chemical resistances to diffusion (R_p and R_c), respectively, as in

$$D_{obs\,f} = \frac{D_{mol}}{R_p R_c} \quad (6)$$

D_{mol} is tabulated for some compounds (*15*) or can be estimated using various empirical relations, for example, the well-known Wilke-Chang equation (*16*). Physical resistance can be equated to a tortuosity factor (τ) that takes into account the winding of pore channels. Tortuosity is difficult to measure, so it may be left as a fitting parameter in diffusion modeling. Since $D_{obs\,f}$ represents diffusion through macropores or mesopores only (defined as internal pores with diameters >2 nm), the constrictivity factor important in hindered diffusion mechanisms in micropores can be neglected (*8*). Tortuosity can be estimated by various empirical relations, such as that proposed by Millington and Quirk (*35*) as used previously (*36*). For fully saturated conditions, this relation gives

$$R_p = \tau = \epsilon^{-1/3} \quad (7)$$

where ϵ is the intraparticle porosity (fraction pores v/v).

The chemical resistance (R_c) can be described as the influence of rapid and reversible partitioning of the labile fraction of PAHs between the sediment and the pore water:

$$R_c = \left(1 + \frac{\rho}{\epsilon}K_{sed-pw}\right) \quad (8)$$

where ρ ($kg\ L^{-1}$) is the sediment bulk density and K_{sed-pw} ($L\ kg^{-1}$) is the sediment−pore water partitioning function. Many other reports have used an analogous representation with a linear K_d to describe sediment−water partitioning of PAHs (*19*, *20*, *23*, *24*). While incorporation of more complex sorption models is possible, including Freundlich (*8*, *10*) or competitive Langmuir (*26*) models, we assume that a linear model is adequate to describe rapid partitioning and diffusion of the labile fraction of PAHs into the intraparticle porewater for the short time periods over which partitioning is important in the model. The use of the directly measured K_{sed-pw} partitioning coefficient is different from previous literature reports and more realistically accounts for the significant portion of PAHs in pore waters that may be associated with dissolved organic carbon (DOC). Combining eqs 7 and 8 with eq 6, we arrive at a predictive expression for fast-domain diffusivity:

$$D_{obs\,f} = \frac{D_{mol}/\epsilon^{-1/3}}{1 + \frac{\rho}{\epsilon}K_{sed-pw}} \quad (9)$$

Finally, eq 9 is substituted into eq 5 to obtain the MOM diffusion model:

$$\frac{M(t)}{M(\infty)} = f\left(1 - \frac{6}{\pi^2}\sum_{n=1}^{\infty}\frac{1}{n^2}\exp\left(-\frac{D_{mol}/\epsilon^{-1/3}}{1+\frac{\rho}{\epsilon}K_{sed-pw}}n^2\pi^2 t/\bar{a}^2\right)\right) + (1-f)\left(1 - \frac{6}{\pi^2}\sum_{n=1}^{\infty}\frac{1}{n^2}\exp(-D_{obs\,s}n^2\pi^2 t/\bar{a}^2)\right) \quad (10)$$

The fraction f was operationally defined as the fraction of total desorbable PAH that is desorbed in 24 h ($M_{24\,h}$) and was confirmed based on statistical correlations between f and $M_{24\,h}$ as described in the text. Therefore, the sole adjustable parameter of the MOM diffusion model is $D_{obs\,s}$.

Results and Discussion

Desorption Trends among PAHs, Sediments, and Fractions. The most striking differences among PAH desorption kinetics from whole and size-fractionated sediments were for different PAH compounds from a given sediment (Figure 1). For example, in NC sediment fractions, the three-ring PAH anthracene desorbed rather slowly; only 25% of the extractable anthracene desorbed in 3 months from each fraction. More anthracene desorbed from PC sediment and size fractions, but most of the desorption occurred almost instantaneously, and the desorption profiles (plots of cumulative desorption with time) were relatively flat and similar in shape to those found in NC fractions. The four-ring PAH pyrene desorbed rapidly and extensively from all sediment fractions in both sediments. For example, in the first day, nearly 50% of the total extractable pyrene desorbed in NC sediment fractions, and more than 75% of the extractable pyrene desorbed in PC sediment fractions. Compared with pyrene, desorption was slower and less extensive for the more hydrophobic PAH benzo[*a*]pyrene (BAP).

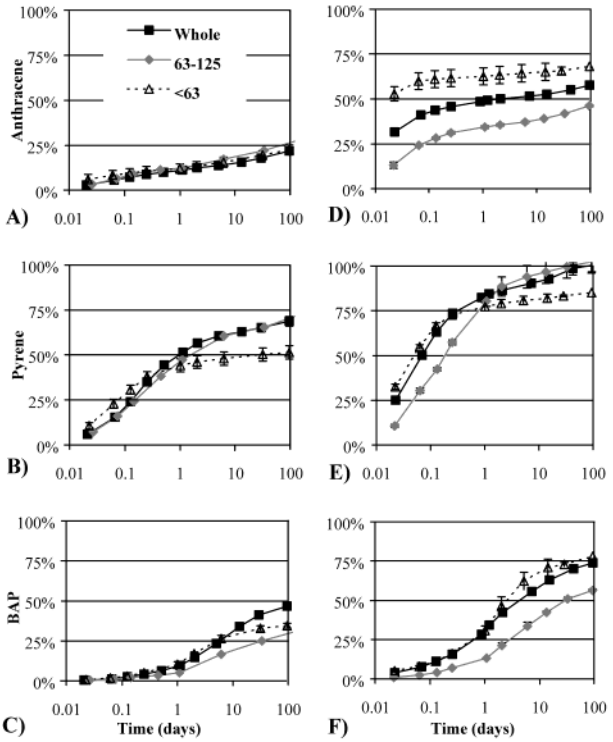

FIGURE 1. Cumulative PAH mass desorbed (as a percent of total extractable mass) for anthracene, pyrene, and BAP from NC whole sediment and size fractions (panels A−C) or from PC whole sediment and fractions (panels D−F). Size fractions are 63−125 and <63 μm. Data reflect mean and range of duplicates.

Comparison of fractional PAH desorption at 1 d (as a percent of the total mass desorbed in 3 months) for a wide range of PAHs shows that pyrene desorbed most rapidly in every sediment fraction of NC sediment and was one of the most rapidly desorbed in PC whole sediment and sediment fractions (Table 1, "A" columns). Anthracene also desorbed rapidly. The behavior of the three-ring PAH phenanthrene was variable; in some cases it desorbed rapidly, and in other instances it desorbed slowly. The four-ring PAHs benz[*a*]anthracene and chrysene always desorbed more slowly than pyrene from every sediment and fraction, and they always desorbed more rapidly than the five-ring compounds benzo[*b*]fluoranthene, benzo[*k*]fluoranthene, and BAP. A generalized ranking of the mass fraction of desorbable PAHs desorbed in 1 d gives pyrene > benz[*a*]anthracene ≈ chrysene > benzo[*b*]fluoranthene ≈ benzo[*k*]fluoranthene ≈ BAP. Trends among other PAHs were ambiguous.

Extent of desorption is defined as the total cumulative desorption in 3 months divided by the total sediment PAH concentration. Overall, pyrene was the most extensively desorbed compound from every sediment and sediment fraction (Table 1, "B" columns). After pyrene, benz[*a*]anthracene and chrysene tended to be the next most readily desorbed PAHs, followed by the five-ring PAHs. BAP tended to be the most extensively desorbed five-ring PAH. The least readily desorbed were the three-ring PAHs anthracene and phenanthrene. A generalized ranking of extent of desorption among all sediment fractions gives pyrene > benz[*a*]anthracene ≈ chrysene > BAP > benzo[*k*]fluoranthene > benzo[*b*]fluoranthene ≈ anthracene > phenanthrene.

There are several interesting trends in this ordering. Notably, the relatively less hydrophobic three-ring compounds anthracene and phenanthrene were the least extensively desorbed, and BAP was extensively desorbed relative to other five-ring PAHs. On the basis of solubility and octanol−water partitioning data (*19*) and previous reports (e.g., ref *37*) we might predict the larger, more hydrophobic PAHs to be less extensively desorbed and the three-ring PAHs to be more extensively desorbed. Consequently, the low extents of desorption for phenanthrene and anthracene may seem anomalous. However, it is important to remember that the sediments in this study were all extensively weathered (*12*). It is likely, therefore, that because the smaller PAHs such as phenanthrene and anthracene are more mobile in the environment and are more readily biodegraded than larger PAHs (*17, 38*), more of the "desorption-labile" fraction of phenanthrene and anthracene may have already been depleted relative to the less biodegradable PAHs. Although significant phenanthrene mass remained in the sediment, this fraction may be sequestered in small pores, trapped in small voids within SOM, or bound in high-energy SOM sites and therefore would be unavailable for desorption but could remain chemically extractable. These findings demonstrate the important potential differences between PAH desorption behavior observed in aged and weathered sediments versus the results we might expect to see in unaged sediments.

Among sediment fractions, extent of desorption was greatest for <63 μm PC sediment. The smallest extent of desorption was from low-density NC sediment. In general, extent of desorption was greater in PC than in NC sediment, greater in high-density than in low-density sediment, greater in fine fractions than in whole sediments, and greater in whole sediments than in 63−125 μm fractions.

Sediment and PAH Properties Correlated with Extent of Desorption. Extent of desorption is a crucial factor in determining the bioavailability and toxicity posed by PAHs within a given sediment. To elucidate the properties that most affect extent of desorption, PAH properties and sediment physical and chemical properties (parameter values available in Table S1) were regressed against extent of desorption after 1 and 90 d for eight PAHs (source data in Table 1; results in Table 2). Because the study sediments are fundamentally different in how they sequester PAHs (*12*), regressions were done separately for NC and PC sediment fractions.

The PAH fraction desorbed at 1 d (as a percentage of total extractable PAH concentration) was highly correlated with PAH properties among NC sediment fractions but not among PC sediment fractions (Table 2). For example, in NC sediment fractions, a significant negative correlation was observed between log K_{ow} and PAH fraction desorbed at 1 d ($p < 0.01$). Extent of desorption at 90 d was not significantly correlated with any PAH property for either study sediment. However, after excluding the more labile and biodegradable compounds phenanthrene and anthracene, highly significant correlations ($p < 0.01$) were found between log K_{ow} and percent desorbed in every case.

Certain sediment physical and chemical properties were significantly correlated with extent of PAH desorption (Table 2). For example, a negative correlation ($p < 0.01$) was found between organic matter (OM) concentration and extent of desorption at 1 d for both PC and NC sediment fractions. This correlation was significant at 90 d desorption for NC sediment fractions but not for PC sediment fractions. The OM to nonsoot carbon ratio (a measure of the degree of chemical reduction of sediment OM (*12*)) was significantly correlated with extent desorption at 1 d for both sediments and for NC fractions at 90 d. In PC sediment, soot carbon concentration was negatively correlated ($p < 0.01$) with extent of desorption at 1 d. However, this correlation was not significant for extent of desorption at 90 d or for NC sediment fractions. Both sediment specific surface area and porosity were significantly correlated with extent of desorption at 1 d for PC sediment fractions but not for NC sediment fractions. No significant correlation was observed between extent of

TABLE 1. Percent PAH Desorption by Compound and Sediment Fraction[a]

	Newtown Creek										Piles Creek					
	whole		63−125 μm		<63 μm		high-ρ		low-ρ		whole		63−125 μm		<63 μm	
	A	B	A	B	A	B	A	B	A	B	A	B	A	B	A	B
phenanthrene	28	12	14	13	60	nd[b]	52	43	50	9	67	59	27	34	nd	nd
anthracene	51	22	45	26	53	23	62	nd	46	11	85	58	74	46	92	68
pyrene	75	69	66	70	86	52	83	51	66	24	84	108	79	102	91	85
benz[*a*]anthracene	51	40	36	39	69	43	73	43	42	22	79	75	64	81	89	84
chrysene	41	24	31	53	68	60	71	54	43	16	76	53	58	67	87	78
benzo[*b*]fluoranthene	21	37	20	18	27	23	31	21	24	15	41	60	23	47	nd	nd
benzo[*k*]fluoranthene	22	41	24	24	37	29	46	23	23	17	51	65	28	51	59	75
benzo[*a*]pyrene	21	47	17	28	31	35	39	31	22	15	47	76	24	57	40	78

[a] Column A, percent desorbed at 1 d as a percent of total desorbed in 3 months. Column B, percent desorbed at 3 months as a percent of the total extractable mass. [b] nd, not determined because of incomplete data.

TABLE 2. Slope of Ordinary Least-Squares Linear Regressions with Intercept for Independent Variables (PAH or Sediment Properties) vs Dependent Variables (Fraction Desorbed or Observed Diffusivity), and Significance (sig)[a] and *p* Value (*p* val) of Slope Terms As Measured by One-Tailed Student's *t*-Test[b]

	Fraction Desorbed[c]							
	NC 1 d		NC 90 d		PC 1 d		PC 90 d	
	slope	sig	slope	sig	slope	sig	slope	sig
PAH log K_{ow}	**−0.06**	***	−0.005		−0.1	*	−0.035	
PAH molecular weight	**−0.002**	***	0.000		−0.0026		−0.001	
PAH HPLC elution time	**−0.009**	***	−0.002		−0.012		−0.0049	
PAH aqueous solubility	0.016		−0.031		−0.13		−0.13	
specific surface area	0.008		0.013		**0.06**	***	0.011	
porosity	−0.007		0.000		**−0.035**	***	0.0001	
OM concn	**−0.001**	***	**−0.001**	***	**−0.001**	***	−0.0007	
soot carbon concn	−0.006	*	−0.004		**−0.012**	***	−0.0042	
soot as % of OC	−0.003		0.005		**−0.029**	***	−0.0045	
OM to nonsoot C ratio	**0.47**	***	**0.58**	***	**−0.59**	**	0.09	

	Observed Diffusivity								
	pD_{obs}[d]			$pD_{obs\,f}$[e]			$pD_{obs\,s}$[e]		
	slope	sig	*p* val	slope	sig	*p* val	slope	sig	*p* val
PAH log K_{ow}	**0.50**	***	2.6E−04	**0.73**	***	2.9E−05	0.0065		0.94
PAH molecular weight	**0.014**	***	3.3E−04	**0.020**	***	3.2E−05	0.0002		0.95
PAH HPLC elution time	**0.065**	***	1.5E−04	**0.10**	***	7.0E−05	0.0030		0.83
PAH aqueous solubility	−0.15		0.68	−0.29		0.22	−0.0061		0.96
specific surface area	**0.20**	***	9.7E−11	**0.10**	***	1.4E−03	**0.066**	***	4.4E−07
porosity	0.037		0.26	**0.087**	***	2.8E−04	**0.050**	***	1.7E−06
OM concn	0.0012		0.64	**0.0048**	**	0.012	**0.0025**	***	4.2E−03
soot carbon concn	**−0.052**	***	9.9E−03	0.016		0.37	0.0051		0.54
soot as % of OC	**−0.070**	***	1.6E−03	−0.017	-	0.37	−0.013		0.15
OM to nonsoot C ratio	**4.6**	***	3.8E−09	**1.77**	**	0.025	**1.2**	***	6.5E−04

[a] Asterisks correspond to significance at the following confidence levels: ***, 99%; **, 95%; *, 90%. Dashes represent correlations at a significance confidence level below 90%. Correlations significant at 95% or greater are shown in boldface type. [b] Independent variable definitions, units, and parameter values can be found in the Supporting Information, Table S1. See the table notes for details on the dependent variables. [c] Fraction of eight PAHs (the same PAHs as are shown in Table 1) desorbed in 1 or 90 d from whole and fractionated Newtown Creek (NC) or Piles Creek (PC) sediment as a percentage of the total extractable PAH mass. [d] Negative log of observed diffusivity (pD_{obs}) fit to desorption kinetics data using the one-domain model. Dependent parameter values in Table 3 for up to 12 three- to six-ring PAHs desorbing from each of eight sediment fractions ($n = 79$). [e] Negative log of fast- and slow-domain observed diffusivity ($pD_{obs\,f}$ and $pD_{obs\,s}$, respectively) fit to desorption kinetics data using the two-domain model. Dependent parameter values in Table 4 for six less hydrophobic PAHs desorbing from each of six sediment fractions ($n = 36$).

desorption and sediment surface area or porosity at 90 d for either PC or NC sediment fractions.

In general, PAH properties were more significantly correlated with desorption from NC sediment fractions than from PC sediment fractions. Conversely, more sediment chemical and physical properties were significantly correlated with extent of desorption from PC sediment fractions but only at 1 d desorption. No significant relationship was found between extent desorption at 90 d from PC sediment fractions and any PAH or sediment independent variable tested. Our results indicate that extent of desorption cannot be easily predicted from characterization data alone. The large differences between physical and chemical characteristics of the two study sediments from the same harbor estuary, coupled with the lack of any clear trends between either sediment's physicochemical properties and extent of desorption, highlight the importance of directly measuring the labile fraction.

Diffusive Mobility Varied Greatly by Sediment Site and Fraction. The one-domain diffusion model (eq 3) represented the experimental desorption data quite well in most cases. Model fits to experimental data are shown for BAP desorption from whole NC and PC sediment and from high- and low-density fractions of NC sediment (Figure 2). The coefficient of determination (R^2) was greater than 0.994 for whole and density-fractionated NC sediment and was 0.983 for whole

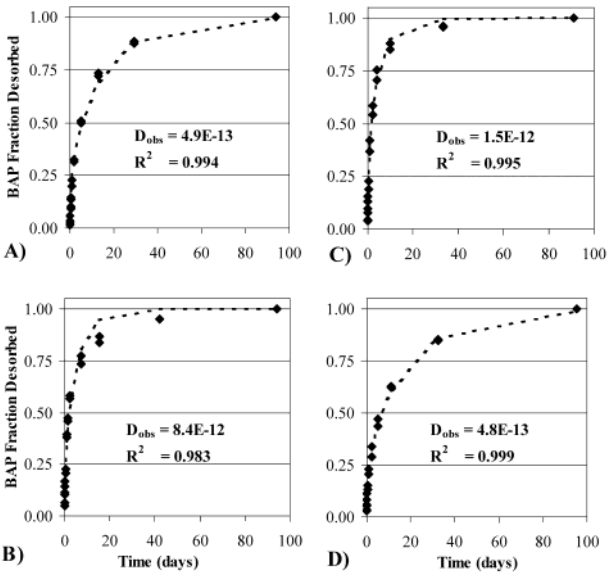

FIGURE 2. One-domain diffusion model fits to BAP desorption kinetics data for (A) whole NC sediment, (B) whole PC sediment, (C) high-density NC sediment, and (D) low-density NC sediment. Also indicated are best-fit observed diffusivity (D_{obs}, cm^2 s^{-1}) and coefficient of determination (R^2).

PC sediment. The observed diffusivity (D_{obs}) for BAP in whole NC and whole PC sediment were 4.9×10^{-13} and 8.4×10^{-12} cm^2 s^{-1}, respectively; 20 times greater in PC than in NC sediment. For all PAHs, diffusivities were higher for PC than for NC sediment (Table 3).

The D_{obs} for BAP from high- and low-density fraction NC sediment were 1.5×10^{-12} and 4.8×10^{-13} cm^2 s^{-1}, respectively (Figure 2). For all PAHs investigated, the ratio of D_{obs} between high- and low-density NC sediment fractions ranged from 2 (for phenanthrene) to 6.3 (for fluoranthene) and averaged about 4 (Table 3). This is consistent with our earlier observation that PAHs desorb faster from high-density than from low-density NC sediment (12). Interestingly, the difference in diffusivity between high- and low-density NC sediment fractions decreased with increasing PAH molecular weight. This result suggests that the mechanism(s) controlling diffusivity for the more hydrophobic PAHs are less sensitive to sediment properties than they are to PAH molecular properties.

D_{obs} values for PAHs in the <63 μm fraction of NC sediment were about 200 times smaller than the corresponding values for PAHs in the 63−125 μm fraction (Table 3). The average ratio of D_{obs} between PC sediment size fractions was 140:1. For both sediments the relative ratio in D_{obs} between fine and 63−125 μm fractions tended to increase with PAH molecular weight. Among all sediment fractions and PAHs, the lowest D_{obs} were found for six-ring PAHs diffusing from the <63 μm fractions. We speculate that the influence of hydrophobicity (or a related property such as molecular diameter) combined with a sediment property of the fine fractions, such as high specific surface area, combine synergistically to dramatically reduce observed diffusivity in these cases.

The ratio of D_{obs} between the <63 μm fractions of PC and NC sediments averaged 5:1 and ranged from parity for six-ring benzo[*g*,*h*,*i*]perylene to over 150:1 for the three-ring PAH anthracene. In general, diffusivities of more hydrophobic PAHs were similar between the fine fractions, but large differences in diffusivity were observed for the less hydrophobic PAHs between the <63 μm fractions of PC and NC sediments. For less hydrophobic PAHs, the mechanism(s) controlling desorption may be sensitive to differences in the sediment physical structure or chemical composition. However, for the most hydrophobic PAHs investigated, a different mechanism that affects desorption equally in the two fine fractions may control diffusivity.

***D_{obs}* Correlated with Log *K_{ow}*, Sediment Surface Area, and OM Properties.** PAH properties and sediment physical and chemical properties were regressed against pD_{obs} (where pD_{obs} = −log D_{obs}) for all PAHs and sediment fractions (n = 79). The results show that the log K_{ow} and molecular weight of the PAHs were positively correlated with pD_{obs} (p = 0.00026 and 0.00033, respectively) (Table 2). The correlation between sediment specific surface area and pD_{obs} was also highly significant ($p = 9.7 \times 10^{-11}$). Surprisingly, OM concentration was not significantly correlated with pD_{obs}; however, the OM composition parameters soot carbon concentration, soot as a percent of organic carbon, and OM to nonsoot C ratio were significantly correlated with pD_{obs} (p = 0.0099, 0.0016, and 3.8×10^{-9}, respectively). The slope of the regression indicated that PAHs diffused faster through sediment fractions with higher soot content. This was not expected based on reports in the literature that soot may represent a particularly strong condensed sorbent for PAHs in sediments (*39*, *40*).

Several regression models also tested correlations between groups of molecular or sediment properties with the dependent variable pD_{obs}. Among all sets of independent variables tested, log K_{ow} and sediment specific surface area were the most significantly correlated with pD_{obs} ($p = 9.8 \times 10^{-7}$ and 5.2×10^{-13}, for log K_{ow} and sediment specific surface area, respectively) (Table S2). Also significantly correlated with pD_{obs} were log K_{ow} and each soot concentration, soot concentration as a percent of organic C concentration, and OM to nonsoot carbon ratio. In conjunction with log K_{ow}, OM concentration was not significantly correlated with pD_{obs}.

A three-independent variable regression model was also tested, which included log K_{ow}, sediment specific surface area, and each OM concentration, soot C concentration, soot as a percent of OM, and OM to nonsoot C ratio. Only for the latter case were all three sets of properties significantly correlated with pD_{obs} ($p = 4 \times 10^{-7}$, 2×10^{-5}, and 4×10^{-3} for log K_{ow}, sediment specific surface area, and OM to nonsoot C ratio, respectively). In a regression model also containing log K_{ow} and sediment specific surface area, the soot parameters were not significantly correlated with pD_{obs}. This result indicates that the inverse relationship between soot concentration and pD_{obs} may be simply result from the autocorrelation between soot concentration and sediment surface area (which was significant: $p = 4 \times 10^{-8}$). The results from these two sediments imply that a diffusion model describing desorption of PAHs should include parameters accounting for PAH hydrophobicity, sediment specific surface area, and the quality, not quantity, of sediment organic matter. These findings would be strengthened by (and suggest a need for) completing similar analyses of additional sediments from a diversity of sites with different sediment physical and chemical characteristics to determine how widely our findings extend.

One-Domain Diffusion Model Results Suggest Desorption Mechanisms. An initial condition explicit in the one-domain diffusion model is the assumption that desorbable PAHs are initially distributed uniformly throughout sediment aggregates. Also, the length scale for diffusion ($\bar{a}$) is defined as the volume-weighted average particle radius for a mixture and was computed a priori from the measured sediment particle size distribution. This length scale is appropriate for diffusion occurring in liquid-filled pores distributed throughout the particle volume (*28*). The success of this model in describing desorption kinetics data for a wide range of PAHs, from sediments from two study sites, and for several sediment fractions (Table 3) supports the validity of these assumptions. In contrast, a previous study reported that PAHs in sand and

TABLE 3. Observed Diffusivity D_{obs} ($cm^2\ s^{-1}$) and Coefficient of Determination (R^2) for One-Domain Spherical Diffusion Model (eq 3) Fit to Desorption Kinetics Data

	whole NC		63−125 μm NC		<63 mm NC		high-ρ NC		low-ρ NC	
	D_{obs}	R^2	D_{obs}	R^2	D_{obs}	R^2	D_{obs}	R^2	D_{obs}	R^2
phenanthrene	3.6E−13	(0.941)	5.3E−13	(0.986)	3.1E−14	(0.91)	3.9E−12	(0.942)	2.0E−12	(0.691)
anthracene	2.1E−12	(0.648)	6.8E−12	(0.907)	1.8E−14	(0.747)	nd[a]	nd	1.4E−12	(0.698)
fluoranthene	7.1E−12	(0.942)	1.7E−11	(0.976)	1.1E−13	(0.931)	2.5E−11	(0.902)	4.0E−12	(0.904)
pyrene	8.0E−12	(0.959)	1.7E−11	(0.984)	1.6E−13	(0.976)	2.6E−11	(0.952)	5.8E−12	(0.959)
benz[*a*]anthracene	1.9E−12	(0.974)	3.4E−12	(0.990)	2.9E−14	(0.987)	6.5E−12	(0.979)	1.5E−12	(0.989)
chrysene	1.1E−12	(0.967)	1.9E−12	(0.983)	3.3E−14	(0.971)	6.1E−12	(0.970)	1.5E−12	(0.983)
benzo[*b*]fluoranthene	5.2E−13	(0.993)	1.3E−12	(0.993)	6.2E−15	(0.988)	1.2E−12	(0.984)	5.3E−13	(0.997)
Benzo[*k*]ffluoranthene	5.5E−13	(0.993)	1.6E−12	(0.994)	8.5E−15	(0.994)	2.1E−12	(0.993)	5.8E−13	(0.998)
benzo[*a*]pyrene	4.9E−13	(0.994)	1.1E−12	(0.993)	6.5E−15	(0.992)	1.6E−12	(0.995)	4.8E−13	(0.999)
benzo[*g*,*h*,*i*]pyrene	nd	nd	2.1E−12	(0.963)	2.7E−15	(0.995)	2.1E−13	(0.972)	nd	nd
indeno[1,2,3-*cd*]pyrene	1.8E−13	(0.982)	4.3E−13	(0.989)	1.7E−15	(0.995)	nd	nd	nd	nd

	whole PC		63−125 μm PC		<63 μm PC	
	D_{obs}	R^2	D_{obs}	R^2	D_{obs}	R^2
phenanthrene	2.9E−11	(0.848)	8.0E−13	(0.923)	nd	nd
anthracene	4.8E−10	(0.207)	8.3E−11	(0.770)	3.0E−12	(0.943)
fluoranthene	1.1E−10	(0.508)	3.5E−11	(0.966)	9.7E−14	(0.852)
pyrene	1.7E−10	(0.821)	3.1E−11	(0.976)	6.4E−13	(0.974)
benz[*a*]anthracene	4.6E−11	(0.968)	1.2E−11	(0.989)	1.9E−13	(0.986)
chrysene	4.2E−11	(0.942)	8.6E−12	(0.979)	2.0E−13	(0.983)
benzo[*b*]fluoranthene	6.3E−12	(0.974)	1.9E−12	(0.992)	nd	nd
benzo[*k*]fluoranthene	9.6E−12	(0.962)	2.2E−12	(0.995)	3.3E−14	(0.99)
benzo[*a*]pyrene	8.4E−12	(0.983)	1.8E−12	(0.995)	1.6E−14	(0.993)
dibenz[*a*,*h*]anthracene	nd	nd	5.9E−13	(0.957)	1.6E−14	(0.964)
benzo[*g*,*h*,*i*]pyrene	nd	nd	1.1E−12	(0.997)	2.6E−15	(0.853)

[a] nd, insufficient data collected to fit diffusivity.

a diagenetically altered coal only existed within 5 μm of the particle surface and suggested that a pore diffusion model may therefore be inappropriate to describe PAH desorption for these particles (*41*). However, the porosity, if any, of these particles was not reported, and so this result may not apply to the porous sediments used in our study.

On the basis of the coefficient of determination values and a qualitative analysis of the residuals, the one-domain model did especially well in describing diffusion of more hydrophobic PAHs from OM-rich sediment fractions. For five- and six-ring PAHs, the median R^2 was >0.99 for all sediment fractions. However, the coefficients of determination were low and variable for phenanthrene and anthracene and in general were lower for less hydrophobic PAHs. The one-domain diffusion model also was not as successful in describing the experimental data for sediments with lower OM content (e.g., high-density NC vs low-density NC sediment, or PC vs NC sediment—as evident in Figure 2). In such cases, another mechanism may control mass transport.

Less Hydrophobic PAHs May Diffuse via Two Distinct Mechanisms. Desorption kinetics for less hydrophobic PAHs (three- and four-ring compounds—corresponding to a log K_{oc} below 6) from whole and fractionated sediments were fit to a two-domain spherical diffusion model (eq 5). The estimated parameter values show that $D_{obs\,f}$ varied significantly among PAHs and sediment fractions, while $D_{obs\,s}$ was less variable (Table 4). $D_{obs\,f}$ ranged from 1.4×10^{-9} $cm^2\ s^{-1}$ for anthracene from whole PC to nearly 500 times smaller: 3.0×10^{-12} $cm^2\ s^{-1}$ for benz[*a*]anthracene from low-density NC sediment. The maximum value for $D_{obs\,s}$ was 2.2×10^{-12} for pyrene desorbing from whole PC sediment, while the minimum value of $D_{obs\,s}$ was 2.1×10^{-13} for benz[*a*]anthracene desorbing from 63−125 μm PC sediment. $D_{obs\,s}$ only varied by a factor of 10 among all 36 combinations of PAHs and sediment fractions. Among sediment fractions, the ratio between $D_{obs\,f}$ and $D_{obs\,s}$ was greatest for the three-ring PAHs phenanthrene and anthracene and least for benz[*a*]anthracene and chrysene. Among PAHs, the ratio between the fast- and slow-domain diffusivity was greater for PC fractions than for NC fractions.

The adjustable parameter *f* describing the fraction of PAH mass in the fast-diffusion domain was highly variable but tended to be smallest for phenanthrene and anthracene and greatest for pyrene (Table 4). This result further supports our previous suggestion that the desorption-labile fraction of phenanthrene and anthracene was already depleted in the sediments. Aside from the behavior of the three-ring PAHs, *f* tended to decrease with increasing hydrophobicity, indicating that a smaller fraction of PAHs was in the fast-diffusion domain. Percent desorbed in 1 d ($M_{24\,h}$) was significantly correlated with *f* ($p = 1.1 \times 10^{-13}$) with a slope close to 1, indicating that $M_{24\,h}$ can be used as a surrogate for *f*. This result was the basis for using the measured 24 h desorbed fraction as the operational definition for *f* in the two-domain MOM diffusion model. If this result is also observed for other HOC contaminants in other sediments, then including a relatively rapid and simple 24 h desorption assay in routine sediment characterization may provide a useful measure of the fraction of total sediment contamination that is readily desorbed, bioavailable, and most likely to affect exposure risk. For the five-and six-ring PAHs, the best-fit *f* was near 0.5 (data not shown) and the fast- and slow-domain diffusivities converged to almost the same value, indicating that even with the additional adjustable parameters, diffusion of more hydrophobic PAHs was well-described by a diffusion model with only a single diffusion domain.

PAH properties and sediment physical and chemical properties were regressed against fast- and slow-domain observed diffusivities. The results show that $pD_{obs\,f}$ was significantly correlated with the log K_{ow} and molecular weight of the PAHs ($p = 2.9 \times 10^{-5}$ and 3.2×10^{-5}, respectively) (Table 2). In contrast, no PAH property was significantly correlated with $pD_{obs\,s}$. These results suggest that the mechanism responsible for the slow-domain diffusivity was not

TABLE 4. Fast- and Slow-Domain Diffusivities ($D_{obs\,f}$, $D_{obs\,s}$ ($cm^2\ s^{-1}$)) and Fraction in Fast Diffusion Domain (f) with Coefficient of Determination (R^2) for Fitting Two-Domain Spherical Diffusion Model (eq 5) to Desorption Kinetics Data for Three- and Four-Ring PAHs

	phenanthrene	anthracene	fluoranthene	pyrene	benz[*a*]anthracene	chrysene
whole NC						
$D_{obs\,f}$	1.9E−11	5.14E−11	1.6E−11	1.5E−11	4.2E−12	3.9E−12
$D_{obs\,s}$	2.1E−13	2.4E−13	3.7E−13	2.9E−13	2.8E−13	2.7E−13
f	0.17	0.42	0.73	0.80	0.68	0.50
R^2	0.987	0.995	0.989	0.990	0.991	0.993
63−125 μm NC						
$D_{obs\,f}$	1.4E−11	1.6E−10	4.0E−11	3.3E−11	5.8E−12	5.9E−12
$D_{obs\,s}$	4.4E−13	6.5E−13	5.0E−13	5.2E−13	4.2E−13	4.6E−13
f	0.08	0.37	0.70	0.76	0.73	0.54
R^2	0.985	0.993	0.993	0.993	0.994	0.992
high-ρ NC						
$D_{obs\,f}$	9.7E−11	1.1E−10	5.9E−11	4.8E−11	1.1E−11	1.3E−11
$D_{obs\,s}$	1.8E−12	3.2E−13	5.0E−13	7.5E−13	4.1E−13	4.3E−13
f	0.26	0.54	0.74	0.79	0.82	0.76
R^2	0.977	0.985	0.978	0.982	0.986	0.987
low-ρ NC						
$D_{obs\,f}$	6.2E−11	7.8E−11	1.9E−11	1.4E−11	3.0E−12	4.2E−12
$D_{obs\,s}$	3.2E−13	3.1E−13	4.2E−13	5.1E−13	3.6E−13	3.8E−13
f	0.39	0.34	0.57	0.70	0.66	0.56
R^2	0.997	0.975	0.996	0.996	0.996	0.997
whole PC						
$D_{obs\,f}$	1.2E−10	1.4E−09	4.8E−10	3.5E−10	7.9E−11	9.5E−11
$D_{obs\,s}$	1.5E−12	1.9E−12	1.8E−12	2.2E−12	1.8E−12	1.9E−12
f	0.62	0.79	0.69	0.80	0.82	0.75
R^2	0.963	0.977	0.889	0.969	0.988	0.984
63−125 μm PC						
$D_{obs\,f}$	2.8E−10	2.9E−10	6.6E−11	5.5E−11	1.6E−11	1.6E−11
$D_{obs\,s}$	5.1E−13	6.6E−13	1.3E−12	1.4E−12	8.0E−13	6.9E−13
f	0.14	0.69	0.80	0.81	0.87	0.77
R^2	0.982	0.987	0.981	0.988	0.992	0.993

significantly influenced by PAH properties. Both $pD_{obs\,f}$ and $pD_{obs\,s}$ were significantly correlated with sediment properties including specific surface area, porosity, OM concentration, and sediment OM to nonsoot ratio. The sediment property most significantly correlated with $pD_{obs\,f}$ was total sediment porosity ($p = 2.8 \times 10^{-4}$), and the sediment property most significantly correlated with $pD_{obs\,s}$ was specific surface area ($p = 4.4 \times 10^{-7}$).

Sets of variables were also tested for correlations with each of $pD_{obs\,f}$ and pD_{obs} *s*. In two independent variable regression models, including $\log K_{ow}$ and each of the sediment properties porosity, specific surface area, OM concentration, and OM to nonsoot C ratio, the independent variables were always significantly correlated with $pD_{obs\,f}$ (Table S3). However, in regression models including $\log K_{ow}$ and each of the same sets of sediment properties, hydrophobicity was not significantly correlated with $pD_{obs\,s}$. These results suggest an important distinction between the mechanisms responsible for fast- versus slow-domain PAH mass transport:

(i) Fast-domain diffusivity is affected by both PAH hydrophobicity and sediment properties.

(ii) Slow-domain diffusivity is affected by only sediment physicochemical properties and not by PAH properties including hydrophobicity.

These results support and extend the findings of a previous study by Ten Hulscher et al. (*42*), who found that the rates of "very slow desorption" of chlorobenzenes, polychlorinated biphenyls, and PAHs from a Netherlands freshwater sediment were very consistent with each other and not a function of compound molecular weight or hydrophobicity, as might be expected.

Validation of the Macro-Mesopore and OM (MOM) Diffusion Model. Desorption kinetics data for phenanthrene, anthracene, and pyrene from both whole sediments were modeled using the MOM diffusion model (eq 10). In this model, $D_{obs\,f}$ was calculated a priori by a set of readily obtainable parameters, including the free aqueous diffusivity of the PAH, the intraparticle porosity and bulk density of the sediment, and the sediment-pore water partitioning coefficient, which is different for each PAH in each sediment. All parameter values are given in Table S1. As described in the Model Development section, $D_{obs\,f}$ is intended to combine sediment−pore water PAH partitioning and aqueous-phase diffusion through the macro-mesopore network of spherical sediment aggregates. Also specified in the MOM diffusion model was the fraction (f) of PAH in the fast-diffusion domain, which was set equal to the fraction of desorbable PAHs that desorbed in 24 h. Therefore, as was the case with the one-domain diffusion model, the MOM diffusion model has one adjustable parameter.

Unlike the one-domain diffusion model, the MOM diffusion model described two distinct diffusive processes responsible for PAH desorption from porous estuarine sediments. The MOM model was more successful in representing the measured desorption kinetics for phenanthrene and pyrene (Figure 3) and for anthracene (Figure S1) from both whole sediments. Comparison of coefficients of determination between the MOM and the one-domain diffusion models confirmed that the MOM model more closely represented the experimental data. We believe that inclusion of a fast-domain macro-mesopore diffusion term in recent PAH sorption−desorption modeling studies may have resulted in better descriptions of the data, where otherwise successful model formulations underpredicted PAH sorption−desorption at short periods of time for less hydrophobic PAHs diffusing through water-saturated porous materials (*14*, *26*).

The adjustable parameter in the MOM model, $D_{obs\,s}$, assumed values between 1.3×10^{-13} $cm^2\,s^{-1}$ for phenanthrene diffusing from whole NC sediment to 1.74×10^{-12} $cm^2\ s^{-1}$ for pyrene diffusing from whole PC sediment. Values for $D_{obs\,s}$ were greater in PC sediment than NC sediment, and the

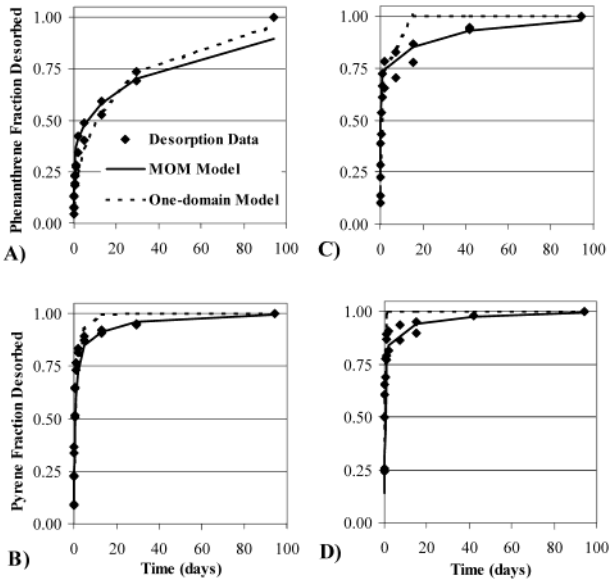

FIGURE 3. Comparison of MOM diffusion model with one-domain diffusion model for representing desorption kinetics data for phenanthrene and pyrene desorbing from whole NC sediment (panels A and B) or from whole PC sediment (panels C and D).

ranking by compound was pyrene > anthracene > phenanthrene for both sediments. The mechanisms controlling the slow-domain diffusivity are the subject of much research and may include micropore blockage by precipitating minerals (*8*), hole filling in void spaces in SOM (*26*), or the presence of high-energy regions in SOM (*7*).

Conceptual Framework for PAH Desorption from Sediment. This study has found that sediment aging history, sediment physical and chemical properties, and PAH properties affect desorption of PAHs from estuarine sediments. On the basis of our findings, we propose a conceptual framework describing intra-aggregate PAH desorption:

(i) Initially, PAHs are distributed throughout sediment aggregates. They may be absorbed in discreet organic matter regions, adsorbed onto hydrophobic coatings along the pore network, and may be found in pore water as freely dissolved PAHs or as PAH−DOC complexes.

(ii) For the most rapid, initial phase of desorption, a significant fraction of less hydrophobic PAHs may be initially in the pore water or be available to rapidly partition into the pore water as either freely dissolved PAHs or as PAH−DOC complexes. This fraction diffuses through the macro-mesopore network and is transported into the bulk or interparticle pore water.

(iii) More hydrophobic PAHs (e.g., log K_{ow} > 6) are less available for rapid partitioning into the pore water, and if they do begin to diffuse through the pore network, they frequently become entrained along hydrophobic pore walls. The dominant diffusion mechanism for more hydrophobic PAHs may be diffusion through OM, which is most affected by the properties of the OM and not by the quantity of OM or by PAH properties.

Correctly understanding and accurately describing the rate, extent, and mechanisms of PAH desorption is crucial for site characterization, optimization of remediation processes, and risk assessment. The results of this study suggest that differences in sediment aging conditions may make it difficult to predict the achievable extent of PAH desorption from fundamental sediment or PAH properties. However, the magnitude of the readily desorbable fraction can be, and possibly should be, measured using a simple 24-h desorption assay. Also, although the mechanism(s) controlling slow-domain diffusivity remain unresolved and are the subject of much current research, pore diffusion may be a key mechanism leading to rapid desorption of relatively less hydrophobic PAHs in systems such as the one explored here. Furthermore, it may be possible to predict the magnitude of the fast-domain diffusivity from readily measured parameters, the most important of these is the sediment−pore water partitioning coefficient. These rapidly desorbing PAHs may also be the most bioavailable component of total sediment PAHs.

Acknowledgments

This work was supported in part by Grant R825303 from the National Center for Environmental Research and Quality Assurance section of the U.S. Environmental Protection Agency, by NOAA Grant NA97OR0338 from the Cooperative Institute for Coastal and Estuarine Environmental Technology, and by Fellowship 5-T32-GM08339 from the National Institutes of Health Rutgers−UMDNJ Biotechnology Training Program. The authors thank three anonymous reviewers for helpful suggestions.

Supporting Information Available

Three tables and one figure. This material is available free of charge via the Internet at http://pubs.acs.org.

Literature Cited

(1) U.S. EPA. *EPA's Contaminated Sediment Management Strategy*; U.S. EPA Office of Water: Washington, DC, 1998; EPA-823-R-98-001.
(2) Hatzinger, P. B.; Alexander, M. *Environ. Sci. Technol.* **1995**, *29*, 537−545.
(3) Nash, R. G.; Woolson, A. E. *Science* **1967**, *157*, 924−927.
(4) Alexander, M. *Environ. Sci. Technol.* **2000**, *34*, 4259−4265.
(5) Shor, L. M.; Kosson, D. S. In *Bioremediation*; Valdes, J. J., Ed.; Kluwer Academic Publishers: Dordrecht, The Netherlands, 2000; pp 15−43.
(6) Pignatello, J. J.; Xing, B. *Environ. Sci. Technol.* **1996**, *30*, 1−11.
(7) Huang, W.; Weber, W. J., Jr. *Environ. Sci. Technol.* **1997**, *31*, 2562−2569.
(8) Farrell, J.; Grassian, D.; Jones, M. *Environ. Sci. Technol.* **1999**, *33*, 1237−1243.
(9) Cornelissen, G.; van Noort, P. C. M.; Govers, H. A. J. *Environ. Sci. Technol.* **1998**, *32*, 3124−3131.
(10) Rügner, H.; Kleineidam, S.; Grathwohl, P. *Environ. Sci. Technol.* **1999**, *33*, 1645−1651.
(11) Nam, K.; Alexander, M. *Environ. Sci. Technol.* **1998**, *32*, 71−74.
(12) Rockne, K. J.; Shor, L. M.; Young, L. Y.; Taghon, G. L.; Kosson, D. S. *Environ. Sci. Technol.* **2002**, *36*, 2636−2644.
(13) LeBoeuf, E. J.; Weber, W. J., Jr. *Environ. Sci. Technol.* **2000**, *34*, 3632−3640.
(14) Ghosh, U.; Talley, J. W.; Luthy, R. G. *Environ. Sci. Technol.* **2001**, *35*, 3468−3475.
(15) Schwarzenbach, R. P.; Gschwend, P. M.; Imboden, D. M. *Environmental Organic Chemistry*; John Wiley & Sons: New York, 1993.
(16) Wilke, C. R.; Chang, P. *AIChE J.* **1955**, *1*, 264−270.
(17) Mackay, D.; Shiu, W. Y.; Ma, K. C. *Illustrated Handbook of Physical−Chemical Properties and Environmental Fate for Organic Chemicals: Vol. II, Polynuclear Aromatic Hydrocarbons, Polychlorinated Dioxins, and Dibenzofurans*; Lewis Publishers: Chelsea, MI, 1992.
(18) Cornelissen, G.; van Noort, P. C. M.; Govers, H. A. J. *Environ. Toxicol. Chem.* **1997**, *16*, 1351−1357.
(19) Wu, S.-C.; Gschwend, P. M. *Environ. Sci. Technol.* **1986**, *20*, 717−725.
(20) Ball, W. P.; Roberts, P. V. *Environ. Sci. Technol.* **1991**, *25*, 1237−1249.
(21) Carroll, K. M.; Harkness, M. R.; Bracco, A. A.; Balcarcel, R. R. *Environ. Sci. Technol.* **1994**, *28*, 253−258.
(22) Rijnaarts, H. H. M.; Bachmann, A.; Jumelet, J. C.; Zehnder, A. J. B. *Environ. Sci. Technol.* **1990**, *24*, 1349−1354.
(23) Scow, K. M.; Huston, J. *Soil Sci. Soc. Am. J.* **1992**, *56*, 119−127.
(24) Ramaswami, A.; Luthy, R. G. *Environ. Sci. Technol.* **1997**, *31*, 2260−2267.
(25) Karapanagioti, H.; Gossard, C.; Strevett, K.; Kolar, R.; Sabatini, D. *J. Contam. Hydrol.* **2001**, *48*, 1−21.

(26) Zhao, D.; Pignatello, J. J.; White, J. C.; Braida, W. *Water Resour. Res.* **2001**, *37*, 2205−2212.
(27) Crank, J. *The Mathematics of Diffusion*; Oxford University Press: Oxford, 1975.
(28) Rao, P. S. C.; Jessup, R. E.; Addiscott, T. M. *Soil Sci.* **1982**, *133*, 342−349.
(29) Cornelissen, G.; van Noort, P. C. M.; Parsons, J. R. *Environ. Sci. Technol.* **1997**, *31*, 454−460.
(30) Kan, A. T.; Chen, W.; Tomson, M. B. *Environ. Pollut.* **2000**, *108*, 81−89.
(31) LeBoeuf, E. J. Ph.D. Dissertation, The University of Michigan, Ann Arbor, MI, 1998.
(32) Steinberg, S. M.; Pignatello, J. J.; Sawhney, B. L. *Environ. Sci. Technol.* **1987**, *21*, 1201−1208.
(33) Farrell, J.; Reinhard, M. *Environ. Sci. Technol.* **1994**, *28*, 63−72.
(34) Schaefer, C. E.; Arands, R. R.; Kosson, D. S. *J. Contam. Hydrol.* **1999**, *40*, 221−238.
(35) Millington, R. J.; Quirk, J. P. *Trans. Faraday Soc.* **1961**, *57*, 1200−1207.
(36) Schaefer, C. E.; Arands, R. R.; vanderSloot, H. A.; Kosson, D. S. *J. Contam. Hydrol.* **1995**, *20*, 145−166.
(37) Helmstetter, M. F.; Alden, R. W. *Arch. Environ. Contam. Toxicol.* **1994**, *26*, 282−291.
(38) Sutherland, J. B.; Rafii, F.; Khan, A. A.; Cerniglia, C. E. In *Microbial Transformation and Degradation of Toxic Organic Chemicals*; Young, L. Y., Cerniglia, C. E., Eds.; Wiley-Liss: New York, 1995; pp 269−306.
(39) Rockne, K. J.; Taghon, G. L.; Kosson, D. S. *Chemosphere* **2000**, *41*, 1125−1135.
(40) Gustafsson, O.; Haghseta, F.; Chan, C. *Environ. Sci. Technol.* **1997**, *31*, 203−209.
(41) Ghosh, U.; Gillette, J. S.; Luthy, R. G.; Zare, R. N. *Environ. Sci. Technol.* **2000**, *34*, 1729−1736.
(42) Ten Hulscher, Th. E. M.; Vrind, B. A.; van den Heuvel, H.; van der Velde, L. E.; van Noort, P. C. M.; Beurskens, J. E. M.; Govers, H. A. J. *Environ. Sci. Technol.* **1999**, *33*, 126−132.

Received for review April 19, 2002. Revised manuscript received January 31, 2003. Accepted February 5, 2003.

ES025734L